Proceedings of the 12th World Congress on Electrical Engineering and Computer Systems and Sciences (EECSS'25)
Paris, France – August 17 - 19, 2025
Paper No. ICBES 181
DOI: 10.11159/icbes25.181

Comparing 3D-Modeling Algorithms to Enhance Remote Diagnosis Accuracy of Psoriasis

Lara Schweickart[1], Julia Hofmann[1], Jan Malte Hustiak[1], Christoph Zimmermann[1], Paul Schöppe[2], Astrid Schmieder[2], Wilhelm Stork[3]
[1]FZI Forschungszentrum Informatik,
Haid-und-Neu-Straße 10-14, Karlsruhe, Germany
schweickart@fzi.de; hofmann2@fzi.de; hustiak@fzi.de; czimmer@fzi.de
[2]Universitätsklinikum Würzburg,
Josef-Schneider-Straße 2, Würzburg, Germany
paul.schoeppe@stud-mail.uni-wuerzburg.de, schmieder_a@ukw.de,
[3]Karlsruher Institut für Technologie,
Kaiserstraße 12, Karlsruhe, Germany
wilhelm.stork@kit.edu

Abstract **-** Telemedicine is playing an ever-increasing role in the field of medicine. The Covid-19 pandemic has shown the great potential and advantages of telemedicine. Dermatology in particular is well suited to the use of telemedicine due to the strong visual component of skin diseases and offers already a wide range of telemedical services. However, studies show that 2D data is not always sufficient for a comparable diagnosis to on-site appointments. This paper therefore investigates the potential of using 3D-models of affected skin to improve diagnostic accuracy. Suitable 3D-modeling algorithms are identified and used with psoriasis data. The modeling algorithms are compared in terms of reconstruction quality and efficiency and evaluated using metric analyses (PSNR, SSIM, L-PIPS), performance data and visual assessments in order to make a final statement about the potential of the investigated algorithms and the use of 3D-models in general for a remote diagnosis improvement of psoriasis diseases.

Keywords**:** telemedicine, dermatology, psoriasis, 3D-modeling

1. Introduction

Rapid advances in digital technologies have significantly impacted healthcare and paved the way for the field of telemedicine. This innovative field enables remote consultations, diagnoses, and treatment plans, reshaping traditional healthcare. The COVID-19 pandemic acted as a catalyst for adoption of telemedical solutions, with restricted physical interactions creating an unprecedented demand for remote healthcare solutions. Due to the visual nature of skin conditions, dermatology is a particularly suitable field for the use of telemedicine, referred to as teledermatology. Teledermatology allows dermatologists to assess skin conditions through images or videos submitted by patients. Several studies underline the efficacy of teledermatology. Diagnostic accuracy rates for teledermatology are reported to be between 75% and 80%, comparable to in-person evaluations [1]. Furthermore, store-and-forward (SAF) teleconsultations have been shown to reduce costs by 18% and avoid 74% of in-person referrals [2]. These benefits make teledermatology a cost-effective and scalable addition to traditional dermatological care.

Despite these advantages, limitations remain. One significant concern is the variability in diagnostic accuracy in different conditions. A study found that psoriasis is 20% less likely to be accurately diagnosed by teledermatology compared to other inflammatory skin diseases [1]. This discrepancy underscores the need for improvements in teledermatology, particularly in conditions with complex visual appearance. A critical limitation of remote consultations is the absence of a three-dimensional (3D) perspective. In on-site examinations, dermatologists rely not only on the appearance of the skin but also on tactile and spatial assessments to evaluate the severity and characteristics of the affected skin. This 3D component is not replicated in current teledermatology applications, often leading to reduced diagnostic precision.

To address these challenges, this paper investigates the feasibility of incorporating 3D-models into teledermatology workflows, specifically the use of video recordings to generate 3D representations of the skin, aiming to bridge the gap between remote and in-person diagnostic accuracy. The focus of this study is on psoriasis, a chronic inflammatory skin

condition that presents unique diagnostic challenges in teledermatology. By leveraging advancements in computer vision and 3D-modeling, we aim to enhance the diagnostic capabilities of teledermatology, contributing to improved patient outcomes and broader adoption of this technology in clinical practice.

2. Related Work

3D-models are widely used in surgical planning to provide patient-specific anatomical representations. 3D printing technology has significantly advanced surgical planning by providing personalized implants and precise preoperative simulations [3].

During the COVID-19 pandemic NASA used holoportation, a technology which creates high-quality 3D-models of people which are then transmitted live and can be displayed with virtual reality devices to create a live-like interaction between remote participants, to enable doctors to examine astronauts in space [4].

Microsoft developed a real-time 3D-telemedicine system for surgical patients. [5] showed that this 3D-telemedicine exceeds 2D-telemedicine especially in the patient satisfaction. While the system still has its limitations and cannot exceed on-site consultations it shows the promising potential of 3D- telemedicine.

While 3D-modeling is used in various fields of medicine, there are currently no approaches in teledermatology which is limited to the transmission of image, video and questionnaire data from the patient to the doctor via corresponding digital health applications.

3. Methodology of 3D-modeling

3.1 Requirements

Together with the possible users requirements for the 3D-modeling were identified. Possible users are mainly dermatologists, so a survey with university dermatologists and independent dermatologists was conducted. Psoriasis patients are not part of the targeted user group, but since their data is used for the system their concerns about the system were also identified during a workshop with patients and their kinsman and transformed into requirements listed in Table I.

Table 1: requirements for 3D-modeling and visualization

ID	**requirement**
R.1	Based on smartphone images
R.2	Short processing time
R.3	Local data processing
R.4	Faithful to original skin
R.5	Viewing from all angles possible
R.6	Zoom-in option
R.7	Ease of use

3.2 Approaches to 3D-modeling based on images

Based on the requirements the three different approaches to 3D-modeling were identified and evaluated. Figure 1 shows the pipeline of the implemented 3D-modeling process.

Preprocessing: For the pipeline input 70 individual images are extracted at equidistant intervals from a 180° video around the object. The videos are from patients who are part of a clinical trial and have visible psoriasis symptoms. A Structure from Motion (SfM) algorithm [6] is used to estimate the camera positions and create a sparse point cloud of the skin area based on the images. The camera positions and sparse dense cloud are used by the Multi-View-Stereo (MVS) algorithm [7] to create a dense point cloud based on the results from the SfM algorithm. The used 3D-modeling methods can create 3D-models based on the data created in preprocessing. The procedure for the approaches is explained below.

Poisson reconstruction [8], aims to transform the dense point cloud from the MVS into a continuous 3D surface. The Poisson reconstruction creates a closed surface that faithfully reproduces the structure and topology of the scene. A surface

is spanned between neighboring points, forming a triangular mesh structure. Both the depth and color information of the dense point cloud is taken into account, resulting in a realistic surface model. The method is based on the solution of the Poisson equation and uses the normal vectors of the dense point cloud to create a continuous surface.

Neural Radiance Fields (NeRF) [9] uses a pre-trained neural network to model the complex light, color and transparency distributions of a scene. By combining geometric information and image data, NeRF can generate a detailed, continuous representation of the scene that also takes reflection effects into account. Objects are modeled by tracing rays from the viewing position. Camera positions and orientations, a sparse point cloud and photographs of the scene from different angles are required to create the model. Based on all input data, the mesh can reconstruct the scene precisely and completely, as both geometric and texture-related information is available. Compared to traditional methods, such as the Poisson reconstruction, NeRF offers a significantly higher visual quality, as it does not use a fixed mesh structure but continuously models volume data [10].

In contrast to NeRF, which is based on neural networks, **Gaussian splatting** uses explicitly stored 3D Gaussian distributions to determine the influence of the points along the rays. These Gaussian distributions are three-dimensional volume elements that are distributed in space and store continuous information about color and transparency. Precise camera parameters and a point cloud form the basis for correctly positioning the Gaussian volume elements in space and determining their attributes. Images of the scene from different angles are also required to optimize the color and transparency information of the Gaussian volume elements. The combination of this input data allows the scene to be represented as a collection of continuously overlapping volume elements [11].

The free availability of these modeling approaches enables local execution on a secure server, which ensures data-protection-compliant processing of the images.

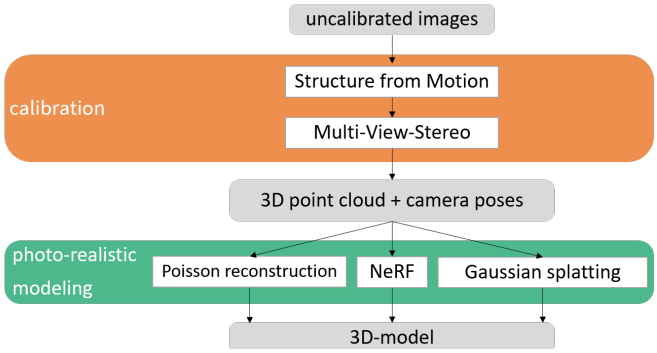

Figure 1: pipeline of 3D-modeling

3.3 Used metrics for evaluation

Three different metrics are used to evaluate the reconstruction quality of the different approaches.

The **peak signal to noise ratio (PNSR)** is a common metric for evaluating reconstruction accuracy. In this context, it is used to analyze the deviation of color brightness values between an original image and the 2D projection generated from the 3D-model [12]. A PSNR value of 30-50 dB is generally regarded as an indicator of a high degree of agreement between the original and the reconstruction [13]. Higher values indicate a smaller deviation, while lower values mean a larger discrepancy.

Structural Similarity (SSIM) is a metric for evaluating the similarity between two images. As an extension to PSNR, SSIM additionally considers brightness, contrast and structure information in order to enable a comparison modelled on human perception [13]. The value range of the result is between 0 and 1. 1 shows maximum similarity between the images, while 0 means a complete deviation [12].

Learned perceptional image patch similarity (L-PIPS) is a metric to evaluate the similarity between images that differs fundamentally from previous mathematical approaches. While PSNR and SSIM are based on numerical or structural comparisons, L-PIPS uses a pre-trained neural network to analyze the semantic and structural similarity of two images. This

approach is modelled on human perception and considers visual aspects that go beyond simple differences in pixels [12]. A value close to 0 means an ideal match and a value of 1 means significant deviations.

4. Results

The three different modeling approaches described above were used on 23 different videos from different patients participating in the study. Image 2 shows the results of the 3D-modeling approaches of three example videos, that capture the advantages and disadvantages identified in the evaluation for all three methods used. For a simplified illustration, an original image and the image of the resulting 3D-models from the different approaches are shown from the same angle. The perspective is chosen so that the psoriasis regions are visible.

4.1 Poisson reconstruction

It is noticeable that the background is displayed incompletely in all images. Due to the smooth surfaces and neutral colors of the materials, there are hardly any concise features that are needed for a complete reconstruction. However, the back of the hand shows a complete reconstruction of the psoriasis regions. No differences are visible in terms of color or the position of the reddish and partially scaly areas. The model of the upper arm shows isolated holes in the surface structure outside the psoriasis region. The overall representation of the model thus loses clarity, but a precise depiction of the psoriasis region is retained. Characteristic features such as plaques and inflammation, which create structured surfaces and clear color boundaries, allow a complete reconstruction of the affected areas. The model of the foot shows isolated artifacts in the psoriasis region. The reconstruction appears complete, but contains serious errors. Reflection artifacts are present on the top

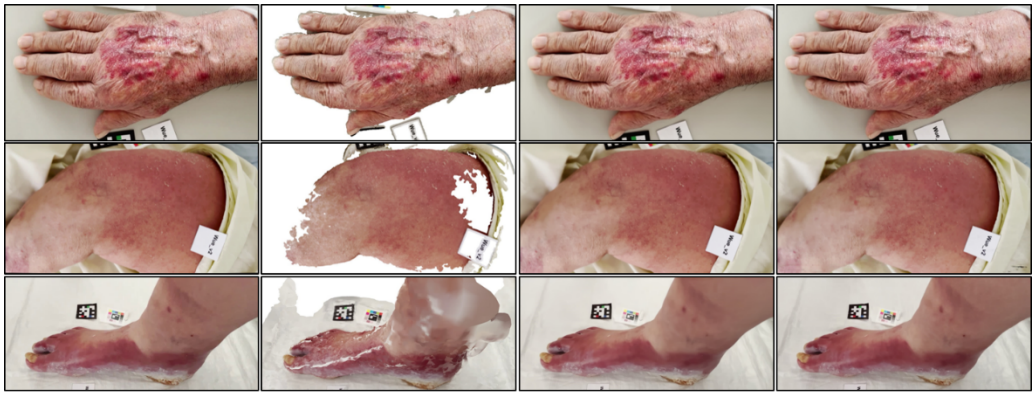

(a) original image (b) Poisson reconstruction (c) NeRF (d) Gaussian splatting

Figure 2: Results of 3D-modeling with different approaches

of the foot.

Excessive illumination from a flat angle of incidence leads to specular reflections, which cause areas of the surface to appear white, and therefore details are lost. The resulting mirror effect is further enhanced by ointments

applied before the image was taken. The metrics calculated in Table II confirm the results of the visual analysis and show the weaknesses of the Poisson reconstruction. The average PSNR is only 12.79 dB. The SSIM also shows a deviation from the ideal value 1 with an average value of 0.67, while the L-PIPS with a result of 0.48 also signals a relatively low similarity. Therefore, the Poisson reconstructions show insufficient accuracy and robustness under different conditions.

Table 2: PSNR, SSIM and L-PIPS of Poisson reconstruction

	PSNR (dB)	SSIM (0-1)	LPIPS (1-0)
ideal value	30-50	1	0
average	12,79	0,67	0,48
back of hand	11,75	0,53	0,42
upper arm	10,99	0,72	0,52
foot	17,25	0,82	0,43

4.2 Neural Radiance Fields

All results show a complete reconstruction of the psoriasis regions. There are no discernible differences to the reference images on the left, both in terms of color and the position of the reddish and partially scaly areas. No holes are visible in the models and even the foot model shows a correct representation of the psoriasis symptoms despite unfavorable lighting conditions. Subjective observation does not reveal any significant differences and the method delivers robust photorealistic results.

Table 3: PSNR, SSIM and L-PIPS of NeRF

	PSNR (dB)	SSIM (0-1)	LPIPS (1-0)
ideal value	30-50	1	0
average	26,27	0,89	0,10
back of hand	23,92	0,74	0,10
upper arm	24,11	0,89	0,14
foot	29,52	0,98	0,07

However, an objective examination of the metrics in Table III shows deviations in the reconstruction quality. For PSNR in particular, neither the average value of 26.27 dB nor any of the individual values are within the ideal range of 30-50 dB. With an average value of 0.89, the SSIM is slightly below the ideal value of 1 and only the foot achieves values greater than 0.9. The L-PIPS achieves a value of 0.09, which is closer to the ideal value of 0. Thus, NeRF objectively achieves a detailed reconstruction, but the metrics indicate slight deviations in the reconstruction.

4.3 Gaussian splatting

Table 4: PSNR, SSIM and L-PIPS of of Gaussian splatting

	PSNR (dB)	SSIM (0-1)	LPIPS (1-0)
ideal value	30-50	1	0
average	33.51	0.98	0.07
back of hand	31.90	0.97	0.07
upper arm	33.64	0.98	0.08
foot	39.35	0.98	0.07

Visually, all results show a complete reconstruction of the psoriasis regions. No differences are discernible in terms of color or the position of the reddish and partially scaly areas. There are no holes in the models and the method delivers robust photorealistic results. Subjective observation does not reveal any significant differences to the reference images on the left.

The objective examination of the metrics in Table IV confirms this. Gaussian splatting is in the ideal range with an average PSNR of 33,51 dB and only the models of the upper arm and foot deviate slightly from the ideal. The average values

of 0.98 for SSIM and 0.07 for L-PIPS are also almost ideal and confirm a detailed reconstruction. The measurements confirm that Gaussian splatting is a particularly robust method that generates efficient results even with varying exposure ratios.

5. Evaluation

From the comparison of the average metrics PSNR, SSIM and L-PIPS of all methods in Table 4, it can be seen that Poisson reconstruction performs significantly worse than NeRF and Gaussian splatting in all quality metrics. As shown in the previous chapter, the results differ greatly from the ideal values, while NeRF and Gaussian splatting achieve almost ideal results. The NeRF and Gaussian splatting models produce more photorealistic images and also fully represent the background compared to Poisson reconstruction. In addition, the psoriasis regions are reconstructed completely and without errors or artefacts. A qualitative evaluation of the NeRF images in Figure 3 with the Gaussian splatting images in Figure 4, recognizes no significant differences between the approaches. However, the metrics in Table 4 show that Gaussian splatting offers advantages over NeRF. With an average of 32.06 dB, the PSNR of Gaussian splatting is the only one in the ideal range of 30-50 dB. The values for SSIM and L-PIPS are also superior at 0.97 and 0.08, compared to NeRF at 0.86 and 0.11. An ideal value of 1 is targeted for the SSIM and 0 for the L- PIPS. Gaussian splatting therefore offers the best results in terms of quality metrics.

In addition to the quality metrics, performance data was collected in order to compare the economic efficiency of the algorithms. The results are shown in Table 4. In terms of performance, Poisson reconstruction offers mixed results. It requires the longest average computing time of 37 minutes 25 seconds and utilizes the GPU processors the most at more than 90 %. However, only a small amount of RAM is required and the model size is the smallest at an average of 37.57 MB. RAM usage averages 0.79 GB, which is the lowest of all models tested. In comparison, NeRF can only achieve better values than Poisson reconstruction in terms of computing time and percentage GPU utilization of 63.93%. With an average of only 13 minutes and 5 seconds per model, NeRF is more than twice as fast as Poisson reconstruction. On the other hand, there is a clear disadvantage in terms of memory requirements. At 4.93 GB, NeRF requires on average more than three times as much memory as the other methods. Furthermore, the generated models are the largest in comparison, with a size of 167 MB. Gaussian splatting, on the other hand, offers the best balance between efficiency and resource utilization. It takes the least time at 12 minutes and 49 seconds, has a low GPU utilization of 63.93%, and the memory requirements of 1.40 GB are significantly lower than those of NeRF. With a model size of 47.20 MB, it is not as compact as the Poisson reconstruction, but still much more efficient.

Table 5: Performance comparison of different methods

Method	**Time** (min:sec)	**GPU Utilization** Ø(%)	**Storage Utilization** Ø(*GB*)	**Size** (MB)	**PSNR** (dB)	**SSIM** (0-1)	**L-PIPS** (1-0)
Poisson reconstruction	37:25	96.02	0.79	37.57	12.99	0.65	0.47
NeRF	13:05	63.93	4.93	167.00	25.08	0.86	0.11
Gaussian splatting	12:49	63.93	1.40	47.20	32.06	0.97	0.08

To summarize, the Poisson reconstruction shows the lowest reconstruction quality, which, however, strongly depends on the quality of the input data. It is susceptible to artefacts, particularly with varying exposure ratios, and is therefore not very robust. It performs worse in the quality metrics than NeRF and Gaussian splatting, but has low memory requirements. NeRF generates complete models of the psoriasis regions and is characterized by a visually high quality. Nevertheless, the memory requirement is a limitation that makes the method less economical, as it requires powerful hardware. Gaussian splatting offers the best performance as it is very fast and places low demands on the computer infrastructure. In addition, it has the highest reconstruction quality according to the metrics used and is therefore the most efficient method.

5.1 User evaluation with dermatologists

In addition, a survey with 16 dermatologists at the University Clinic of Würzburg was conducted. The dermatologists were presented with the four 3D-models created by Gaussian splatting and 2D images of the same areas taken by the patients. They were then asked to complete a questionnaire to evaluate both approaches to remote diagnosis.

The results of the survey show a clear preference for 3D-models over 2D photographs in the dermatological assessment of psoriatic skin lesions. All 16 participants stated that 3D-models were clearer than 2D photos. On a scale of 1 to 5, with 5 being the best, recognition of skin changes was rated an average of 4.7, level of detail of skin structure 4.2, and recognition of transitions between healthy and affected skin 4.6. The ability to view skin changes from different perspectives (4.8) and better assessment of plaque elevation (4.3) were particularly noted. In addition, These values are visualized in Image 3. 16 out of 16 respondents found 3D-models to be more accurate in assessing disease severity and helpful for remote treatment (4.8). The usability of the system was rated using the System Usability Scale (SUS) developed by John Brooke [14], which enables a quantitative analysis of the usability. The survey resulted in a SUS score of 80.63, which is generally considered an "excellent" usability and often qualifies as an A grade in usability benchmarking. In conclusion, the results show that 3D-models provide significant added value for clinical diagnosis and treatment planning and would be preferred for remote diagnosis and therapy adjustment.

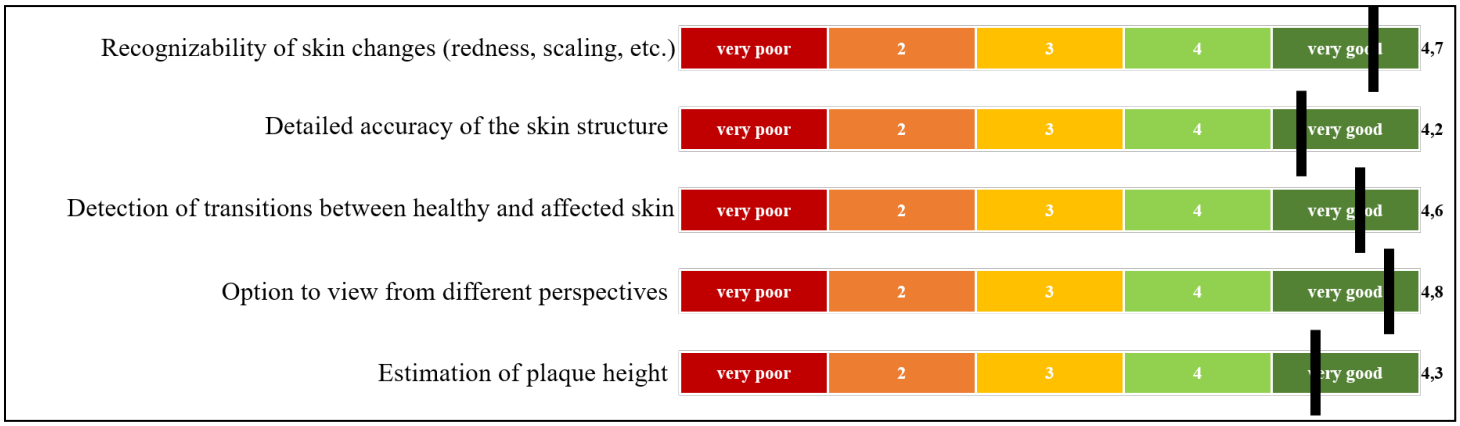

Figure 3: Evaluation results

5.2 Evaluation of the requirements

The proposed 3D-modeling approach successfully meets all predefined requirements for the reconstruction of psoriatic skin from smartphone images. The approach is based on smartphone images the patients can take by themselves at home (R.1). The processing time for generating a 3D-model is 13 minutes (R.2), ensuring a rapid turnaround suitable for clinical applications. To maintain data privacy, all processing is performed on a local server, eliminating the need for external data transmission (R.3). The generated models accurately capture the morphology and texture of the skin, as indicated by quantitative metrics (R.4). Furthermore, the models allow for unrestricted viewing from all angles (R.5) and include a zoom-in function for detailed inspection of affected areas (R.6).

Usability assessments yielded a SUS score of 80,63, indicating a high level of user-friendliness and intuitive interaction (R.7). These results confirm that the developed 3D-modeling pipeline is both technically robust and clinically viable for remote dermatological assessment.

6. Conclusion and Outlook

The use of 3D-models and innovative tactile and virtual interfaces should enable remote medical assessments of the disease.

To this end, methods for creating 3D-models of affected skin areas based on uncalibrated images from ordinary smartphone cameras were presented and compared in this paper. This approach aims to simplify the imaging process for

patients and avoid privacy violations by performing all calculations locally on protected servers. The methods Poisson reconstruction, NeRF and Gaussian splatting were used. The results were evaluated in terms of reconstruction accuracy and performance using the PSNR, SSIM and L-PIPS metrics. Gaussian splatting delivered the best results and is characterized by high precision and robustness. The models enable a visual assessment of the disease symptoms thanks to their photorealistic representation.

In summary, the work shows that the use of photorealistic 3D-models, especially through Gaussian splatting, offers potential to improve telemedical treatment. The advantages of viewing skin areas with flexible perspectives can help dermatologists to assess psoriasis and make a correct diagnosis.

References

[1] N. Nami, C. Massone, P. Rubegni, G. Cevenini, M. Fimiani, and R. Hofmann-Wellenhof, "Concordance and time estimation of store- and-forward mobile teledermatology compared to classical face-to-face consultation," Acta Dermato-Venereologica, vol. 95, 2015.

[2] J. J. Lee and J. C. English 3rd., "Teledermatology: A review and update," American Journal of Clinical Dermatology, vol. 19, pp. 253–260, 2018.

[3] M. Pfeiffer, H. Kenngott, A. Preukschas, M. Huber, L. Bettscheider, B. Müller-Stich, and S. Speidel, "Imhotep: Virtual reality framework for surgical applications," International Journal of Computer Assisted Radiology and Surgery, vol. 13, pp. 741–748, 2018.

[4] M. A. Garcia. (2022, May 8) Innovative 3d telemedicine to help keep astronauts healthy. [Online]. Available: https://www.nasa.gov/humans-in- space/innovative-3d-telemedicine-to-help-keep-astronauts-healthy/?utm

[5] S. Lo, S. Fowers, K. Darko, T. Spina, C. Graham, A. Britto, A. Rose, D. Tittsworth, A. McIntyre, C. O'Dowd, R. Maguire, W. Chang, D. Young, A. Hoak, R. Young, M. Dunlop, L. Ankrah, M. Messow, O. Ampomah, B. Cutler, R. Armstrong, R. Lalwani, R. Davison, S. Bagnall, W. Hudson, M. Shepperd, and J. Johnson, "Participatory development of a 3d telemedicine system during covid: The future of remote consultations," Journal of Plastic, Reconstructive & Aesthetic Surgery, vol. 87, pp. 479–490, 2023.

[6] J. L. Schönberger and J.-M. Frahm, "Structure-from-motion revisited," in Conference on Computer Vision and Pattern Recognition (CVPR), 2016.

[7] J. L. Schönberger, "Robust methods for accurate and efficient 3d modeling from unstructured imagery," Ph.D. dissertation, ETH Zürich, 2018.

[8] M. Kazhdan and H. Hoppe, "Screened poisson surface reconstruction," ACM Transactions on Graphics, vol. 32, no. 3, pp. 1–13, 2013.

[9] M. Tancik, E. Weber, E. Ng, R. Li, B. Yi, T. Wang, A. Kristoffersen, J. Austin, K. Salahi, A. Ahuja, D. Mcallister, J. Kerr, and A. Kanazawa, "Nerfstudio: A modular framework for neural radiance field development," in SIGGRAPH '23 Conference Proceedings, Los Angeles, CA, USA, 2023, pp. 1–12.

[10] B. Mildenhall, P. P. Srinivasan, M. Tancik, J. T. Barron, R. Ramamoorthi, and R. Ng, "Nerf: Representing scenes as neural radiance fields for view synthesis," Communications of the ACM, vol. 65, no. 1, pp. 99–106, 2022.

[11] T. Wu, Y.-J. Yuan, L.-X. Zhang, J. Yang, Y.-P. Cao, L.-Q. Yan, and L. Gao, "Recent advances in 3d gaussian splatting," Computational Visual Media, vol. 10, no. 4, pp. 613–642, 2024.

[12] R. Zhang, P. Isola, A. A. Efros, E. Shechtman, and O. Wang, "The unreasonable effectiveness of deep features as a perceptual metric," in Proceedings of the IEEE Conference on Computer Vision and Pattern Recognition (CVPR), 2018, pp. 586–595.

[13] A. C. Bovik, Handbook of Image and Video Processing, 2nd ed. San Diego, CA, USA: Academic Press, 2005.

[14] J. Brooke, "SUS – a quick and dirty usability scale," 1995.